

Performance of the Accelerating Cavities at the Superconducting Darmstadt Linear Accelerator (S - DALINAC) *)

K. Alrutz - Ziemssen, D. Flasche, H.-D. Gräf, V. Huck, M. Knirsch, W. Lotz,
A. Richter, T. Rietdorf, P. Schardt, E. Spamer, A. Stascheck, O. Titze, W. Voigt
H. Weise and W. Ziegler

Institut für Kernphysik, Technische Hochschule Darmstadt,
Schlossgartenstrasse 9, D - 6100 Darmstadt, Germany

I. Introduction

The 10 MeV injector of the superconducting 130 MeV electron accelerator at Darmstadt (S - DALINAC) produced its first beam in August 87 [1] when a phase locked operation of its 5 - cell capture section and two 20 - cell structures was achieved for the first time. Status reports have been presented after the installation of the first [2] and the second cryomodule of the main linac [3] each one containing two 20 - cell accelerating structures. Therefore only a brief description of the accelerator recalling its main design parameters and its present status of installation is given in Sect. II. Results from some 550 hours of machine time for accelerator tests and from 950 hours of injector beamtime for atomic and nuclear physics experiments are summarized in Sect. III.

Main emphasis however is laid on the experience we gained during this time with the performance of the superconducting cavities (Sect. IV) and associated equipment (Sect.V) like couplers , tuners and windows. The development of a modest infrastructure for cavity treatment is still in progress. Section VI therefore describes the present status of installations and how we intend to improve them. It also contains an outlook on how we will proceed in the completion of the accelerator.

II. Present Status

The main design parameters of the accelerator are summarized in Tab. I below.

Table I: Design parameters of the accelerator

Beam energy / MeV		10 - 130
Energy spread / keV		± 13
cw current / μ A		≥ 20
Operating frequency / MHz		2997
Number of structures	1.00 m long	10
Capture section	0.25 m long	1

*) Work supported by the Bundesministerium für Forschung und Technologie of the Federal Republik of Germany (contract number O6 DA 184 I)

A schematic layout of the accelerator is shown in Fig. 1. Preformation of the bunches is performed at room temperature (right upper portion of the figure). A dc electron beam of 250 keV is first chopped into segments corresponding to 30° of rf phase and then compressed by a prebuncher into 6° when it enters the superconducting part of the accelerator. The 10 MeV injector consists of a 5 - cell capture section (0.25 m long) in a short cryogenic module and two 20 - cell accelerating structures (1 m long) in a standard cryomodule. The main linac (center portion of Fig. 1) consists of four cryomodules housing eight 20 - cell structures and increases the beam energy by 40 MeV. Two transport systems each consisting of two isochronous 180° bends (like the injection into the main linac) and two straight sections allow for two recirculations of the beam, increasing the energy to a maximum of 130 MeV.

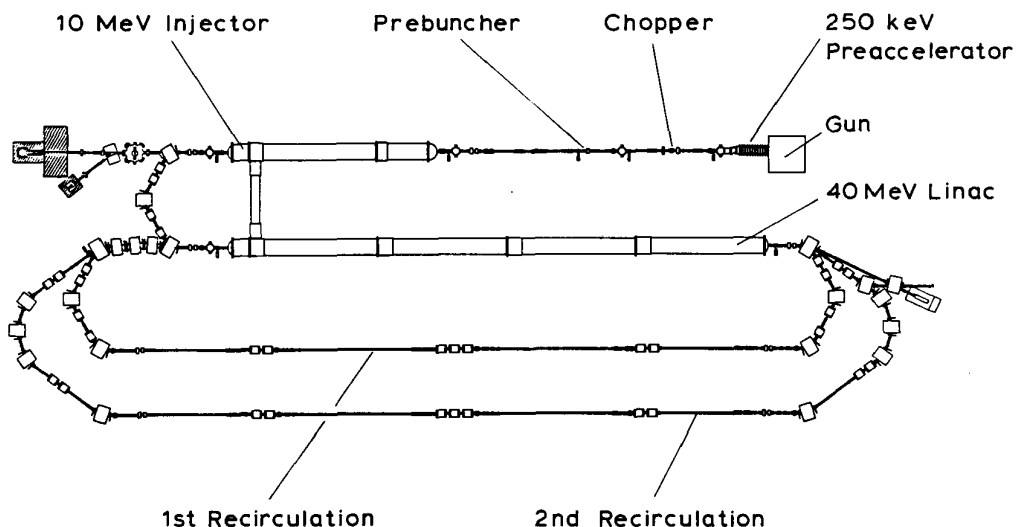


Fig. 1 Layout of the S - DALINAC

Extraction of the beam to the experimental areas is indicated in the extreme right portion of Fig. 1 whereas the upper left portion shows two experimental facilities which use the straight ahead beam of the injector, one for the investigation of channeling radiation and one for nuclear resonance fluorescence experiments.

The status of installation is as follows: the injector linac is in operation since some two years and has been used for experiments rather extensively. Three (out of four) cryomodules of the main linac containing six accelerating structures are installed. The two recirculating beam transport systems are ready for use and the beam has been transported back the first recirculation. It could however not be recirculated through the main linac for reasons which will be explained in Sect. III. The installation of the beam transport from the accelerator extraction to the experimental facilities in the neighbouring experimental area (to the right of Fig. 1) is presently being completed. The system will be available for the next test period. A view of the accelerator as seen from the lower left corner of Fig. 1 is shown in Fig. 2. The injector linac is hidden almost completely behind the three modules of the main linac which dominates the center portion of the picture. The straight

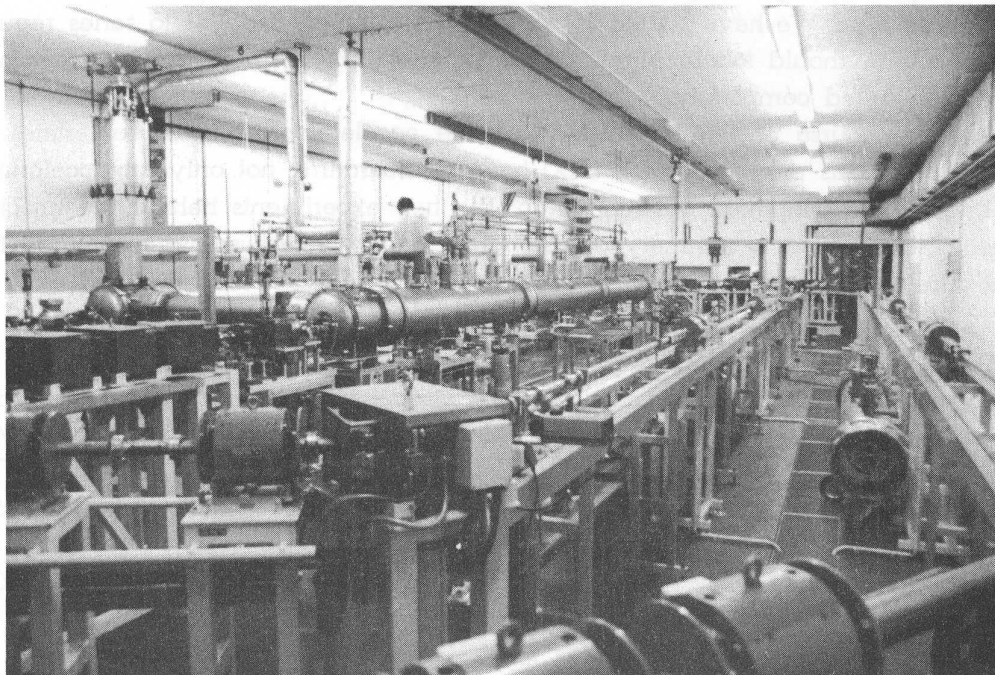


Fig. 2 *View of the main linac and the recirculation beam lines*

sections of the recirculating beamlines are heading towards the spectator and some of the magnets of the 180° bends and of the chicane necessary for the reinjection of the beam into the main linac are visible in the foreground whereas the remaining two 180° bends and the extraction are located at the far end of the hall. The fourth cryomodule of the linac (still to be installed) is sitting on the floor beside the beamline of the second recirculation. The upper left portion of the picture shows the valve box connecting the cryostat system of the accelerator via a short transfer line with the refrigerator located on the other side of the left wall and the LN_2 supply line for the radiation shields of the cryostat.

III. Accelerator Operation and Tests

The main obstacle that had to be overcome before a successful operation of the accelerator could be achieved was the development of the rf control circuits. As reported earlier [1] circuits similar to those described in Ref. [4] allowed the first operation of the injector linac and are still used to control amplitude and phase of the three structures contained in this part of the accelerator. In the meantime a new computer controlled system (its principle of operation, which closely follows the ideas of Ref. [5], has already been presented at the 3rd Workshop [1]), has been tested successfully [2,3] and the six structures of the main linac are controlled by these circuits. Presently a phase stability of better than 1° with respect to an external reference is achieved in accordance with the design figures

of the accelerator. The amplitude is controlled to within $\pm 3 \cdot 10^{-3}$ only, a fact which is mainly due to pick up from the klystron power supplies which are of the switching type. We have started to convert these power supplies to series regulation which should totally eliminate the pick up but the first prototype has not yet been tested completely.

In the course of the last two years the accelerator in its different states of construction has produced some 1500 hours of beamtime not only for accelerator testing and development but mainly for the two experiments behind the injector linac. Table 2 gives a summary of beamtime, energy range and current used for the different purposes.

Table 2: Beam for experiments

Experiment	Energy / MeV	Current / μ A	Time / h
Channeling Radiation	3.0 - 7.7	0.001 - 30	250
Nuclear Resonance Fluorescence	2.5 - 8.5	20 - 40	700
Accelerator Test and Development	1.0 - 9.1	0.1 - 40	550

It has to be noted that the time when the beam was used for atomic and nuclear physics experiments (mostly during nights and weekends) provided very valuable information about the performance and the reliability of the accelerator. The nuclear resonance fluorescence experiment required rather high beam currents because of the small cross sections involved. It was very encouraging that currents of 20 - 40 μ A could be obtained without major difficulties. The beam spot size at the exit window (about 5 m downstream the beamline) was only 4 - 5 mm in diameter and remained that way even for running periods of several days. The channeling radiation experiment always requires excellent beam quality because of the small acceptance angle of the crystals used as targets. The beam always met the requirements without any collimation or focusing between the accelerator and the target. The measurements started with very low beam currents (several nA) because the experiment was strictly limited by the counting rate of the Si(Li) detector positioned at 0° with respect to the beam axis. This summer with different detection techniques the experiment could use a current of up to 30 μ A and no measurable degradation of the beam quality could be observed.

Up to now malfunction of components associated with the superconducting cavities (see Sect. V) prevented an acceleration test using all of the installed cavities simultaneously. In most cases some of the mechanical coarse tuners quit working and prevented to tune all of the cavities to the proper operating frequency. On two occasions a leak from the helium system into the cavity vacuum (partial pressure $\approx 5 \cdot 10^{-5}$ mPa) did not allow a phase locked operation. Therefore only tests using different combinations of accelerating structures in the injector and the main linac as reported earlier [3] have been carried out.

During the most recent test period this summer again a leak in the main linac, which started as a "superleak" and developed into an ordinary leak later on did not allow a phase locked operation of the accelerating structures contained therein. Nevertheless some important results could be obtained: i) Due to an improved gradient of the second 20 - cell structure the energy of the injector increased to 9.1 MeV. ii) A 6.8 MeV beam from the injector was injected into the main linac and transmitted through all of its six cavities. Without further acceleration the beam size at the end of the linac could be kept smaller than 5 mm by proper adjustment of the optics of the injection bend. Using three viewscreens, one in front of the main linac, one at its exit (12.2 m downstream) and one in front of the first dipole magnet of the extraction (another 3.3 m downstream), to determine the beamsizes enabled us to calculate an upper limit of the beam emittance. Horizontally beam diameters of 3.1, 1.9 and 2.2 mm were measured on the respective screens, yielding an emittance of $\epsilon_x = 0.11 \pm 0.03 \pi \cdot \text{mm} \cdot \text{mrad}$. In the vertical direction beam spot diameters of 2.7, 3.8 and 4.8 mm give $\epsilon_y = 0.21 \pm 0.03 \pi \cdot \text{mm} \cdot \text{mrad}$. This number contains some contribution from a small vertical deflection of the beam, the origin of which could not be localized yet. iii) The beam was also sent through the first 180° bend of the first recirculation and transported back the straight section of this beamline. Again the beamsizes were observed at the beginning at the center and at the end of the straight beamline and by proper adjustment of the quadrupoles the diameter could be kept to within 3 mm at all three observation positions.

In order to reinject the recirculated beam into the linac its momentum has to be five times that of the injector beam. Because of the reasons mentioned above (not enough cavities in a phase locked condition) the energy gain of the main linac has not yet been high enough to match that ratio for reasonable injector energies. Also the phase slip of the bunches travelling through the first recirculation becomes prohibitively large for energies below 20 MeV.

IV. Cavity Performance

The gradients of the cavities summarized in Tab. 3 below have been obtained in two ways by rf measurements (figures labeled "rf") following the techniques described in Ref. [7] and by measuring the energy gain of the electron beam (figures labeled "exp") with a deflection magnet (either a 40° bending magnet behind the injector which is part of the channeling radiation experiment or the first dipole magnet of the extraction system behind the main linac).

On a first glance the gradients look rather disappointing compared with modern standards but one has to recall the fact that the cavities have been fabricated almost 6 years ago, most of them from reactor grade (RRR ≈ 30) material. The average gradient of these cavities amounts to 2.2 MV/m and is much lower than the corresponding figure for the three samples made from RRR = 100 niobium which amounts to 5.1 MV/m. The third cavity in the injector is the first one of the 20 - cell structures that exceeds the design figure of 5 MV/m. This has been achieved after an intermediate chemical polishing ($\approx 10 \mu\text{m}$) of the cavity at the University of Wuppertal.

In the meantime we have ordered six cavities manufactured from high purity (RRR ≈ 280) material to replace the cavities with the lowest gradients presently installed.

Table 3: Fields of superconducting cavities

#	Type	Location	RRR	$E_{acc} / MV/m$	
				(exp)	(rf)
1	5 cell	Injector	100	5.5	5.5
2	20 cell	Injector	30	2.0	2.1
3	20 cell	Injector	100	6.3	7.5
4	20 cell	Linac	30	2.2	—
5	20 cell	Linac	30	0.9	0.9
6	20 cell	Linac	30	4.5	4.9
7	20 cell	Linac	30	2.0	2.7
8	20 cell	Linac	30	1.4	—
9	20 cell	Linac	100	3.4	—

The reason for an extremely poor performance of a cavity (like e.g. the second cavity of the main linac) is very probably a "defect" like the one in Fig. 3.

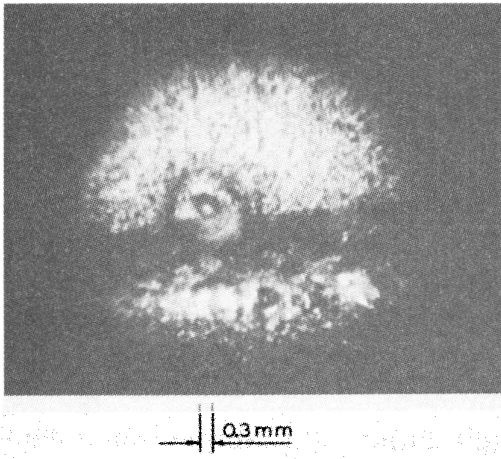


Fig. 3 Defect near the equator weld inside the 9th cell of a 20-cell cavity

This "bad spot" is located close to the equator weld inside the 9th cell of a 20-cell structure which has also been limited to a gradient of 1 MV/m. The "spot" consists of a little crater, 0.3 mm in diameter, inside a shiny area (1.3 mm in diameter) surrounded by a dark halo. "Defects" of a similar appearance have been found occasionally in reactor grade niobium.

The discrepancy between the figures derived from beam energies and the ones from rf measurements are mainly due to two reasons: i) For the rf measurements the cavities were powered to a field level as high as possible, just before a quench

occured. It is however in general not possible to operate a structure for several hours in a phase locked condition at this high field level. ii) The rf measurements were performed on the cavities installed in the accelerator with a strongly over-coupled input which together with reflections from the isolator at the output of the klystron reduces the accuracy of the measurement.

V. Associated Equipment

As already mentioned malfunction of components directly associated with the cavities did not allow acceleration of the beam by all of the installed accelerating structures and prevented recirculation of the beam. Figure 4 shows a cross section of the 5 - cell capture section (3) equipped with rf input (1) and output coupler (5), mechanical coarse tuner (2) and piezoelectric elements (4) for fine tuning. The cavity itself is located inside a titanium tube and every second cell rests on a small adjustable plate (6). In the upper part of Fig. 5 a 20 - cell structure with - out couplers and tuners is shown whereas in the lower part of the picture another cavity is equipped with these devices. The cold window is part of the input coup - ler (mounted to the left cutoff tube of the cavity). A second window (at room temperature) is located at the upper end of the 7/8" coaxial input line (above the input coupler). In the course of the last two years it turned out that after several cycles from room temperature to 2 K and back the ceramic windows in the input couplers, which separate the cavity vacuum from the insulating vacuum of the cryostat, start to develop small leaks. We therefore consider to separate the

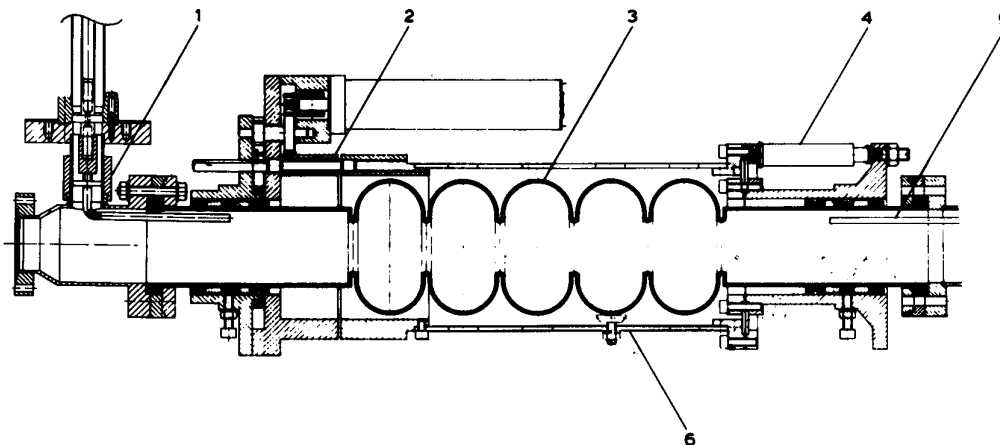


Fig. 4 Cross section of a 5 - cell cavity with tuners and rf couplers

coaxial input line from the insulating vacuum and make its inside part of the cavity vacuum. The output coupler uses a commercial ceramic type N feedthrough welded into a small CF flange. Three of these feedthroughs became heavily leak - ing during cooldown (at temperatures between 4 K and 20 K) requiring time consuming immediate replacement. The mechanical coarse tuner changes the length of the cavity by means of three differential screws driven by a planetary gear which is connected to a dc motor by another planetary gear with a speed re - duction of 1:1750. All of the moving mechanical parts of the tuners are carefully degreased, lubricated with MoS₂ and run in at LN₂ temperature before being in - stalled in the accelerator. Nevertheless they show a rather short lifetime on the average (during the last test period five out of nine tuners became inoperational). Therefore we have started the development of a new tuner in spring this year and a first prototype shown in Fig. 6 is almost ready for testing. The tuner consists of a

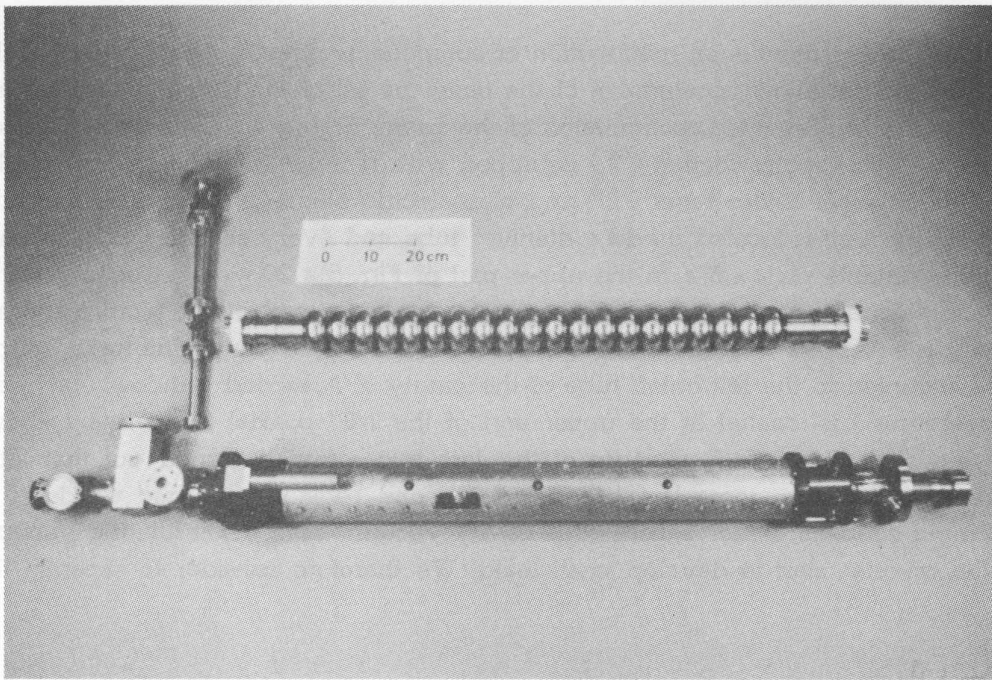


Fig. 5 20 - cell cavity with and without rf input line, tuners and rf couplers

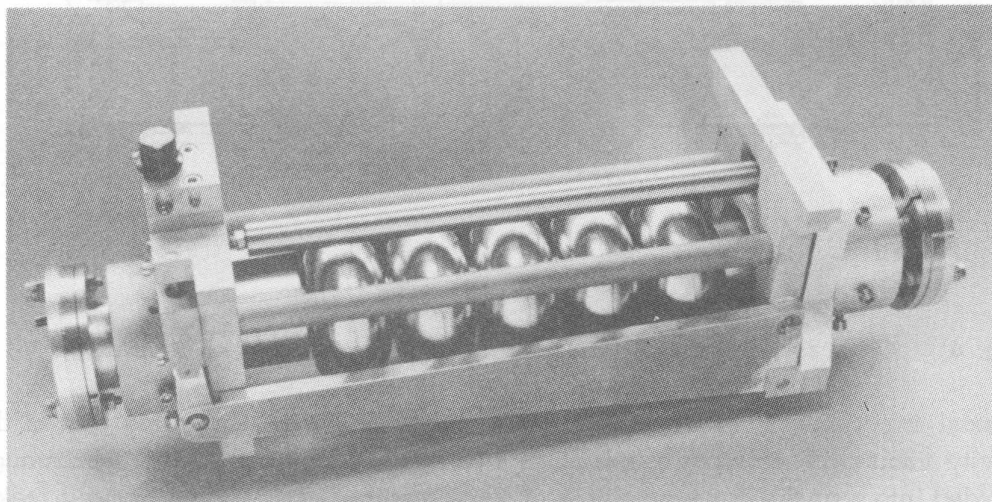


Fig. 6 First prototype of the newly developed tuner

mainframe (the two inner plates fixed to each other by four titanium rods, one of which is visible in Fig. 6). The left cutoff tube of the cavity is fixed to the left plate and the cells of the cavity rest on the lower two titanium rods. The right cutoff tube of the cavity is fixed to a cylindrical part which is pushed against a movable plate by the spring action of the cavity. Two stainless steel balls allow angular movements between the plate and the cylindrical piece. The plate in its upper part pushes against a magnetostrictive rod, a design that has been developed

more than one year ago [3] and has been tested extensively in the meantime. The lower part of the moving plate is connected to a lever on each side which reduces the spring force of the cavity by a factor of ten. A vertically moving part to the left of the mainframe, guided by two linear ball bearings actuated by a ball screw in the center is connected to the levers and moves them up and down, providing a tuning range of 1 MHz while the magnetostrictive rod will allow fine tuning over a range of 4 kHz. The shaft of the ball screw will be extended to a rotary feedthrough at the top of the cryostat. The motor and reduction gear will be outside of the cryostat.

VI. Outlook

Besides the developments mentioned in the previous section we are presently trying to improve the infrastructure for cavity inspection, treatment and repair. An optical inspection facility has been built where the cavity can be moved precisely over a rotatable shaft which carries a mirror with proper illumination. A telescope equipped with an x - y measuring device is inspecting the cavity interior via the mirror. The photograph of Fig. 3 was obtained with this device. During the next couple of months a commercial endoscope will be added to the apparatus to make it even more flexible.

When the optical parts of the device are replaced by a string with a bead aligned to the axis of the cavity precise measurements of field profiles can be obtained. Reliable measurements of the π mode do however still present a problem because of its overlap with the $19\pi/20$ mode. Excitation of the cavity from both sides with a carefully balanced amplitude and phase relationship allows to excite odd or even modes of the TM_{010} passband selectively. A "beadpull" measurement even with extremely small perturbation seems to destroy the balance and yields nonreliable results for the π mode. The left part of Fig. 7 therefore shows typical measurements of field profiles of other modes of this passband. The observed asymmetries are due to imperfections of individual cells.

Using the full 20 - cell geometry as input to the URMEL code we have performed extensive calculations to obtain the field profiles and power distributions in the 20 modes of the TM_{010} passband and to study the effect of any single detuned cell in a 20 - cell accelerating structure. The results enable us to calculate field profiles and power distributions for any combination of detuned cells. The right part of Fig. 7 shows the result of such a calculation where it has been assumed that cells # 19 and # 20 are detuned by ± 9.7 MHz, respectively. A comparison between the measured and the calculated field profiles shown in Fig. 7 yields that the extremely simple assumption of only two cells being detuned describes the gross features of the observed asymmetries rather well, details of course are still missed. The final goal of these studies is to invert the calculations in order to be able to determine the detuning of individual cells from measured field profiles and to find the location of "bad" cells from measurements of the quality factor of an installed cavity in different modes as a kind of in situ diagnostics.

For ultrasonic cleaning of cavities a device has been installed which vertically moves the head of an ultrasound transmitter along the axis of the cavity. The process takes one hour for a 20 - cell cavity. When the ultrasonic equipment is re -

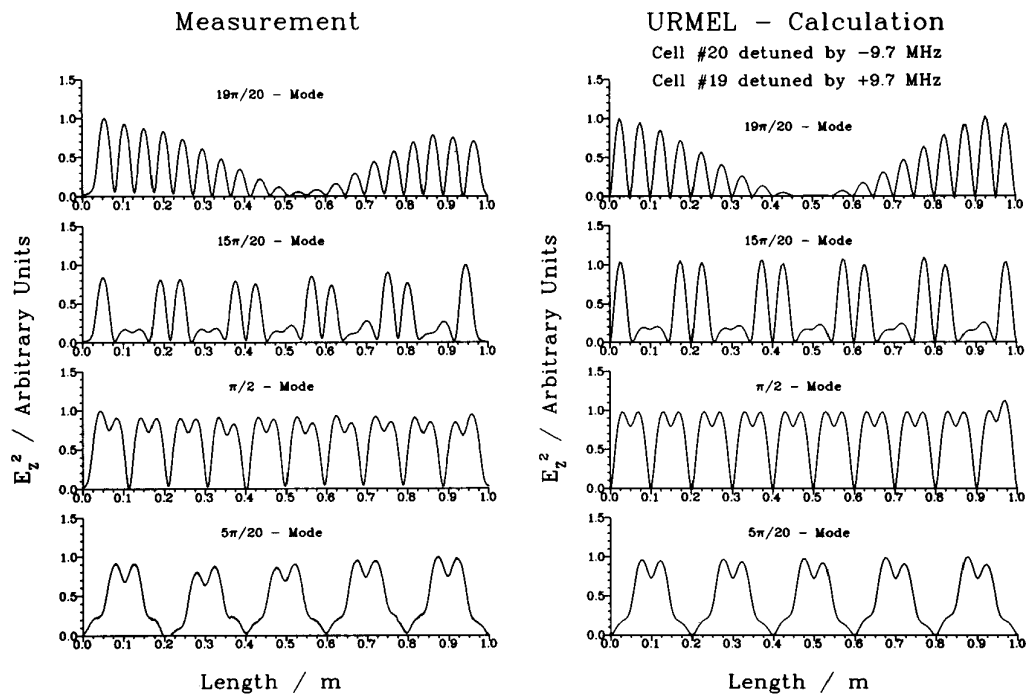


Fig. 7 Measured field profiles of members of the TM_{010} passband of a 20-cell cavity (left) compared with a calculation (right) assuming two detuned cells.

placed by a teflon head which sprays demineralized water in a disclike pattern the same machine can be used for cavity rinsing. We also started to plan the installation of a facility for "soft" chemistry, i.e. buffered chemical polishing but the realization of this project will of course take several months.

In the construction of the accelerator we will proceed as follows: the main linac will be disconnected cryogenically from the injector because some repair work has to be performed on each of the three modules presently installed. The mechanical coarse tuner at the capture section in the injector will be repaired and then the injector will be cooled down in order to deliver beam to the experiments while the modules of the main linac are worked on and while the fourth module will be equipped with another two accelerating structures. Finally after warm up of the injector all four modules of the linac will be installed and during the following test period we hope not only to recirculate the beam for the first time but also to extract it to the spectrometer area for electron scattering experiments.

Acknowledgement

The accelerator is the result of a very fruitful collaboration with H. Piel and his group from the physics department of the University of Wuppertal. The still continuing help of H. Heinrichs and J. Pouryamont is gratefully acknowledged. We feel very obliged to H. Lengler for his continuous support by fruitful discussions

and help with equipment. Stimulating discussions with J.M. Cavedon, J. R. Delayen, P. Leconte, A. Matheisen, D. Proch, A. Schwettman, I. Secutovicz, K. Shepard and W. Weingarten have been very helpful in the course of the project. We feel indebted to B. Aune and A. Mosnier for their generous help with ideas and equipment. Without T. Weiland and his group the very extensive use of their codes on our computers would have been impossible. We are very grateful for the tremendous help provided by the technical staff at the S - DALINAC and the mechanical and electronic workshops of the institutions at Wuppertal and Darmstadt.

References

- [1] V. Aab, K. Alrutz - Ziemsen, R. Amend, D. Flasche, H. - D. Gräf, V. Huck, K.D. Hummel, M. Knirsch, F. Lindqvist, W. Lotz, A. Richter, T. Rietdorf, U. Schaaf, S. Simrock, E. Spamer, A. Stiller, O. Titze, H. Weise, W. Ziegler, H. Heinrichs, H. Piel, J. Pouryamont,
Proc. Third Workshop on RF Superconductivity, ANL - PHY - 88 - 1, Argonne, Ill., USA (1988) 127.
- [2] V. Aab, K. Alrutz - Ziemsen, R. Amend, D. Flasche, H. - D. Gräf, V. Huck, K.D. Hummel, M. Knirsch, F. Lindqvist, W. Lotz, A. Richter, T. Rietdorf, U. Schaaf, S. Simrock, E. Spamer, A. Stiller, O. Titze, H. Weise, W. Ziegler, H. Heinrichs, H. Piel, J. Pouryamont,
Proc. 1988 Europ. Part. Acc. Conf., June 7 - 11. 1988, Rome, Italy
- [3] H. - D. Gräf, A. Richter, Proc. 1988 Lin. Acc. Conf., October 3 - 7, 1988, Williamsburg, VA, USA (to be published).
- [4] I. Ben - Zvi, M. Birk, C. Broude, G. Gitlitz, M. Sidi, J. S. Sokolowski, J.M. Brennan, Nucl. Instr. A 245 (1986) 1.
- [5] J.R. Delayen, G.J. Dick, J.E. Mercereau, IEEE Trans. Nucl. Sci. NS - 24. No. 3 (1977) 1759.
- [6] W. Lotz, H. Genz, A. Richter, W. Knüpfer, J.P.F. Sellschop, J. Physique, C9, (1987) 95.
- [7] H. Piel, Proc. First Workshop on RF Superconductivity, KfK 3019, Karlsruhe, Fed. Rep. of Germany (1980) 85.